J Mater Sci (2006) 41:4643–4648
DOI 10.1007/s10853-006-0059-y

Some aspects of the fracture behaviour of $Mg_{65}Cu_{25}Y_{10}$ bulk metallic glass during room-temperature bending

G. Chen · M. Ferry

Received: 18 January 2005 / Accepted: 19 September 2005 / Published online: 4 May 2006

Abstract The fracture behaviour of $Mg_{65}Cu_{25}Y_{10}$ bulk metallic glass (BMG) during room-temperature three-point bending was investigated. The BMG was initially produced by casting into a wedge-shaped mold which generated an amorphous structure below the ~4 mm thickness zone of the wedge. Three-point bend testing was then carried out on the BMG with the fracture angles and salient features of the fracture surfaces examined by scanning electron microscopy. Observations indicate that this type of deformation mode results in fracture via crack propagation from both surfaces of the samples where the tensile and compressive stresses are greatest. The direction of crack propagation was also found to deviate considerably from 45° to the length direction of sample. A scanning electron microscopy (SEM) study of the fracture surfaces indicated that deformation banding was a feature of crack propagation within compressive zone whereas the tensile zone generated a featureless surface characteristic of brittle failure. The mechanism of failure of the present alloy is discussed on the basis of the observed features on the fracture surfaces and the direction of propagation of cracks during failure and compared with the failure mechanism of samples fractured under both simple tension and compression.

G. Chen (✉)
School of Materials Science and Engineering, Jiangsu University, Zhenjiang 212013, P.R. China
e-mail: gchen@ujs.edu.cn

M. Ferry
School of Materials Science and Engineering, University of New South Wales, Sydney, NSW 2052, Australia

Introduction

Bulk metallic glasses (BMGs) have shown potential as structure materials due to their attractive mechanical properties, but several practical applications are limited by their lack of plasticity [1]. The deformation and fracture behaviour of metallic glasses has been widely investigated [1–12]. In general, the plastic deformation of a metallic glass is localised within narrow shear bands, followed by the rapid propagation of these bands leading to sudden fracture. Under a compressive load, metallic glasses deform and fracture along localised shear bands and the fracture angle between the compressive axis and the shear plane, θ_C, is generally less than 45° (42–43°) [12]. However, under tensile loading, the fracture angle between the tensile axis and the shear plane, θ_T, is generally found to be larger than 45°, and in the range of 50–65°, with an average value of 56° [12].

Zhang et al. [12] recently investigated the compressive and tensile fracture behaviour of a $Zr_{59}Cu_{20}Al_{10}Ni_8Ti_3$ BMG and observed a deviation of crack propagation from 45° of both θ_C and θ_T. Such an effect was argued to be a result of a combined effect of the normal and shear stresses on the fracture plane during crack propagation. Consequently, fracture in these and other materials does not appear to occur along the maximum shear stress plane under both compressive and tensile loading. It is pertinent to note, however, that less research has been carried out on the fracture behaviour of BMGs during deformation processes that generate both principal compressive and tensile stresses in a given sample. In cases such as tensile deformation of notched samples [11], the complex stress state generated within the sample may strongly influence the deformation and fracture behaviour of the BMG [11].

Recent work has shown that Mg-based amorphous alloys can be produced in rod form with a diameter of up to

~4 mm by conventional casting methods [13]; a discovery that is expected to stimulate further research into this new type of high-strength bulk lightweight alloy. A useful outcome of the discovery of Mg-base BMGs is their large supercooled liquid region (ΔT_x) which can be exploited to allow for large strain deformation processing, since this temperature interval can result in superplastic deformation by ideal Newtonian flow [14, 15]. Nevertheless, very little has been published concerning the deformation behaviour of Mg-base BMGs at room temperature, particularly in the presence of a complex stress state. In the present paper, three-point bending was carried out on an amorphous $Mg_{65}Cu_{25}Y_{10}$ alloy at room temperature to investigate its fracture behaviour under a more complex deformation condition than is associated with both simple tension and compression.

Experimental procedure

An alloy of composition (at.%) $Mg_{65}Cu_{25}Y_{10}$ was produced in ingot form by melting high purity magnesium (99.98 wt.%) and a Cu–Y master alloy in an electrical resistance furnace in an argon atmosphere. The Cu–Y master alloy was initially prepared by arc melting high-purity copper and yttrium (99.99 wt.%). Wedge-shaped samples [16] of a width of 40 mm were prepared by conventional mold casting. Previous work has shown that, for this alloy composition, the maximum thickness of the casting that generates a completely amorphous state is ~4 mm [17] which is similar to that observed for cylindrical castings [13].

The as-cast samples were sectioned below the 4 mm thickness zone of the wedge and machined and polished to produce rectangular samples of size 15 mm × 2 mm × 1 mm. A Philips X1400 X-ray diffractometer was used to examine the phase constituents of samples after casting. In order to eliminate the probable influence of surface oxidation, all the samples were mechanically polished before carrying out XRD. Five specimens were prepared for three-point bend testing using a MTS servohydraulic testing machine at a punch velocity of 5×10^{-4} m/s. A schematic diagram of the bending procedure is shown in Fig. 1. The fracture angles, i.e., the angles between the loading axis, as well as the fracture surfaces were examined by scanning electron microscopy (SEM) using a Hitachi S4500 field emission gun (FEG) SEM.

Results and discussion

Figure 2 shows a typical XRD spectrum of an as-cast sample which is similar in form to several other

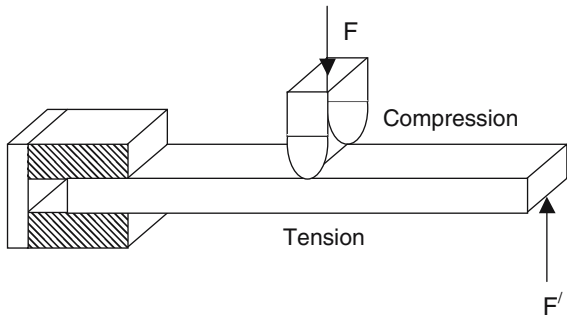

Fig. 1 Schematic diagram of the experimental set-up for three-point bend testing

investigations [13, 16, 17] and confirms that the alloy is amorphous. Recent work has shown that this amorphous structure crystallizes to produce a successive range of crystalline phases including Mg_2Cu, $Mg_{24}Y_5$ and Cu_2Y on reheating [17].

Unlike uniaxial tension and compression, three-point bending induces a high gradient in stress state through the thickness of the sample whereby the face of loading experiences a compressive stress but which decreases to a neutral point at the mid-thickness of the section where the transverse shear stress is maximum through to a pure tensile stress at the opposite face [18]. Figure 3 is a typical load–displacement curve of the three-point bend test of $Mg_{65}Cu_{25}Y_{10}$ BMG. The load–displacement curve is linear up to the point of failure, which indicates elastic deformation is predominant, but this is followed by a small drop in load prior to failure. The bend strength of this specimen was calculated to be ~560 MPa, which is close to the tensile strength of the alloy. Figure 4 shows an SEM micrograph of the transverse section of a sample fractured during mechanical testing. The surfaces are shown by the dashed horizontal lines with the direction of crack propagation relative to the sample surfaces clearly seen. The diagram in Fig. 4b is a schematic of the entire fracture surface showing the areas examined by SEM (A–D). For a

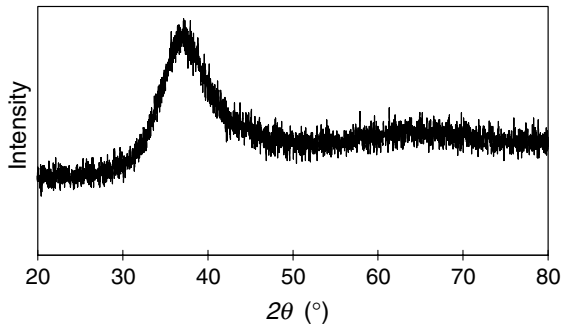

Fig. 2 XRD spectrum of the as-cast alloy taken below the 4 mm thickness point of a casting produced in a wedge-shaped mold showing the characteristic profile of an amorphous alloy

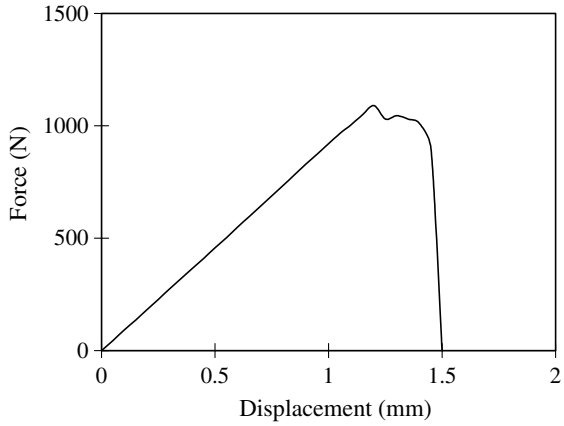

Fig. 3 Load–displacement curve from a typical three-point bend test of the BMG, tested at a punch velocity of ~5×10^{-4} m/s

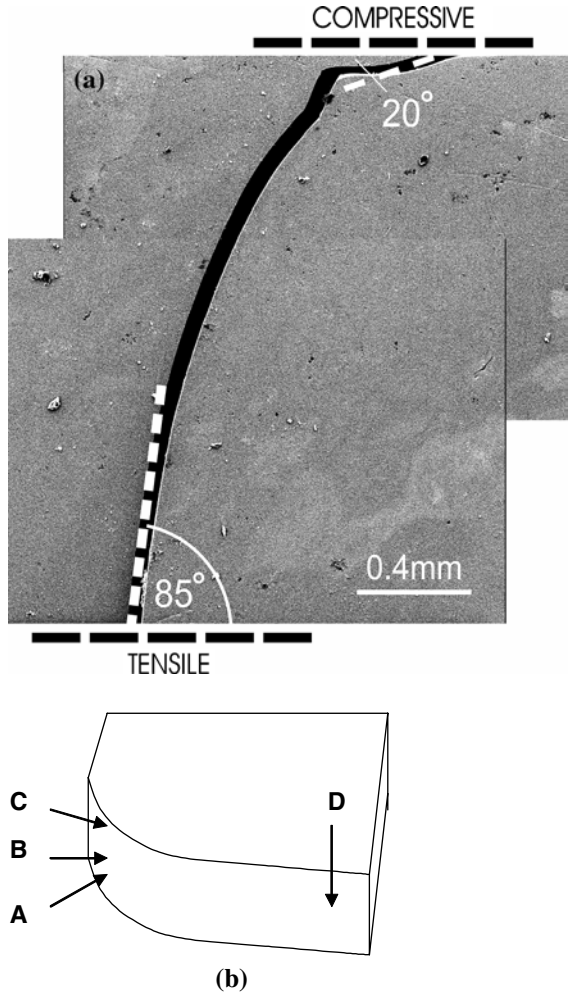

Fig. 4 (**a**) SEM micrograph of the side view of a fractured sample after testing indicating the direction of crack propagation as a function of stress state (tensile at the top and compressive at the bottom). (**b**) Schematic diagram of the fracture surface where A–D are indicated in the text

given failed sample, the crack angle was found to change through the thickness direction of test piece. Figure 4a shows a typical example where the angle between the fracture surface and the axis of loading was ~80–90° at the opposite face to loading (bottom surface) which deviates to 20–40° at the top surface. The values of θ in bending therefore differ to that for a range of metallic glasses in pure tension (θ_T = 50–65°) and pure compression (θ_C = 42°) (see e.g. Tables 1 and 2 in ref. 12) and confirms the complex stress state during bending. Overall, a crack is most likely to initiate at the surface that experiences a pure tensile stress state and will propagate perpendicular to the surface [19]. Due to the compressive stress state within the upper half of a sample, the crack appears to deviate towards 45° to the load axis, which is the expected value for pure compressive deformation of a material that follows the von Mises criterion [18]. In three-point bending tests, the first fracture results from the interaction between the gradient of the stress field induced and the distribution of the fracture stresses through the test specimens [19].

Figure 5 shows a series SEM micrographs of a region that experiences a compressive stress state (region A–C in Fig. 4b). Figure 5a, b show the general morphology of the fracture surface where striations associated with deformation banding are evident. The deformation bands are similar in morphology to that observed by He et al. [20] in Zr-base BMGs deformed in compression and have the form of localised protuberances (arrowed in Fig. 5b) with a band spacing of up to 20 μm. Figure 5c and the higher magnification micrograph of Fig. 5d show a deformed step in region B with deformation bands. Figure 6 shows some further SEM micrographs taken at region C which clearly shows localised deformation banding. SEM micrographs of a region that experiences a tensile stress state (D) are shown in Fig. 7. In this region, the fracture surface is characterised by an essentially featureless morphology but Fig. 7b shows the presence of fine striations on the fracture surface.

Similar to amorphous alloys in the form of thin ribbons, BMGs often fail at low deformation temperature through the formation of shear bands which propagate catastrophically due to material's lack of structure that characterises a dislocation-containing crystalline metal which can undergo extensive plastic deformation and work hardening [21]. Early work on the fracture behaviour of metallic glasses showed that voids and vein patterns were usually present on the fracture surfaces, which implies that flow processes are active which may subsequently result in fracture by microvoid coalescence [7–10]. However, no evidence of voids or vein-like patterns was found in the fractured samples of the present Mg alloy following three-point bending. The notable features of the fracture surface, particularly in the compressive region (Fig. 5), indicate

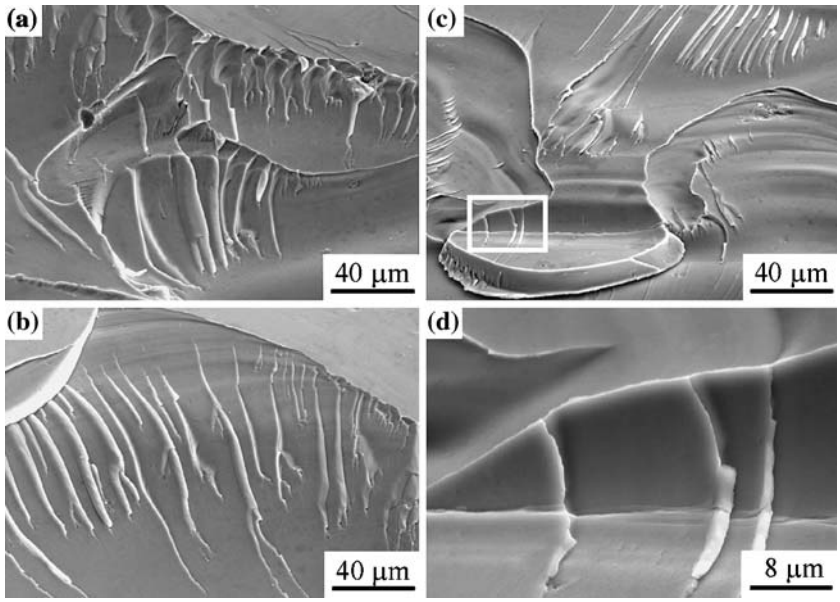

Fig. 5 SEM micrographs of the fracture surface in (the compressive) region A (**a** and **b**) and B (**c** and **d**) of Fig. 4b showing various deformation features

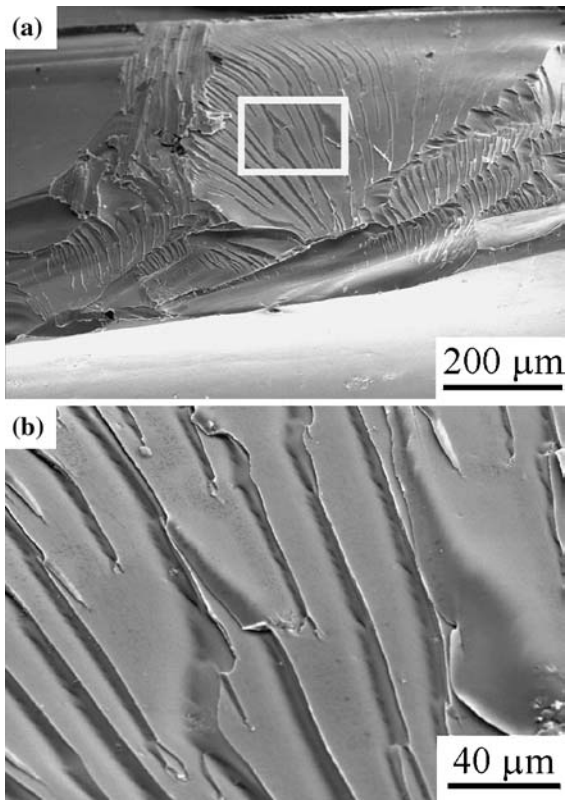

Fig. 6 SEM micrographs of the fracture surface in region C of Fig. 4b

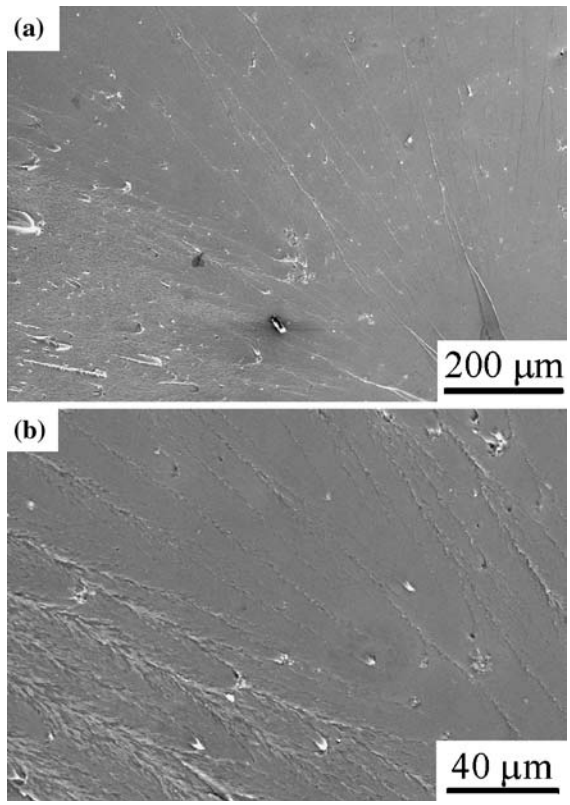

Fig. 7 SEM micrographs of the fracture surface in (the tensile) region D of Fig. 4b showing an essentially featureless morphology

that substantial localised deformation banding occurs. Such a phenomenon is probably a consequence of the high strength, large elastic energy and low melting temperature of this amorphous alloy which are common characteristics of some BMGs [20].

Under compressive loading, there is evidence that the deformation bands that form can partially melt [11, 20] which may result in a condition of reduced friction between the sliding surfaces. The partial melting observed by He et al. [20] was argued to be a result of the high

local increases in temperature during deformation due to the characteristic high strength and large elastic strain energy of BMGs. It has been shown that the temperature rise (ΔT) associated with the propagation of a crack tip may be well up to 280 °C which is dependent on the thermal expansion coefficient, bulk modulus and local stress state of the material [11, 22, 23]. It has also been reported that deformation-induced nanocrystallization can occur in an Al-based amorphous alloy at temperatures below ambient [24]. For the present alloy, the glass transition, crystallization and melting temperatures are ~140 °C, ~200 °C and ~450 °C, respectively [17]. Hence, the temperature rise within a deformation band may result in either Newtonian plastic flow [18] or melting due to the high local stress state at the crack front. Under conditions of either localised melting ($>T_m$) or Newtonian plastic flow ($>T_g$), the normal stress will subsequently decrease via the decrease in friction which will subsequently increase the ease of sliding of the fracture surfaces. Hence, it is likely that the angle between the loading axis and the sliding direction, θ, will be substantially decreased. As θdecreases, however, the effective shear stress,τ, will also increase thereby reducing the ease of sliding. The optimum condition will result in a value of θ somewhat below 45^o due to the decrease in friction whereas τ increases by only a small value. Under tensile loading, however, the initiation of failure occurs at an effective shear stress, τ, which is essentially the same value as for compression [12]. The difference both in the direction of crack propagation and fracture surfaces between regions of sample undergoing either compressive and tensile loading is that, in the latter, cores and veins may be produced at a certain normal stress with eventual failure occurring under a co-operative combination of shear and normal stresses [12]. It is likely that crack initiation occurs in the vicinity of the tensile surface of sample during bending with the stress state across the flexing sample no longer comparable with the uncracked state. Hence, the crack-tip stress fields are expected to govern the crack path. It is pertinent to point out, however, that the crack-tip stress will be affected by the loading stress in the specimen [25–29]. Therefore, bending may result in crack initiation on one or both sides of the sample, as indicated in Fig. 1, that results in crack propagation at an angle of ~90° on the tensile side that approaches less than 45° on the compressive side of the sample.

Conclusions

A $Mg_{65}Cu_{25}Y_{10}$ BMG was produced by casting into a wedge-shaped mold which generated a completely amorphous structure in the alloy for section sizes below ~4 mm. The ambient temperature deformation behaviour of the BMG was studied by three-point bend testing. The following conclusions can be made: (i) unlike pure tension or compression, there is a considerable deviation of the crack angle from 45° to the stress axis for both the compressive and tensile sides of the sample; (ii) There is evidence of plastic deformation on the side of the sample that experiences a compressive stress state, as characterised by deformation bands on the fracture surface which is possibly a result of the high strength, large elastic energy and low melting temperature of the Mg-base metallic glass, and (iii) For a range of samples, crack propagation followed a consistent path, which provides evidence that the final fracture plane is a result of the interaction between the gradient of the stress field and the distribution of the fracture stresses through the test specimens.

Acknowledgement One of the authors, G. Chen, would like to acknowledge the School of Materials Science and Engineering, UNSW for use of their research facilities and the Chinese Scholarship Council for financial support. Both authors gratefully thank Mr Bülent Gun and Mr Kevin Laws for their help with the casting experiments.

References

1. Inoue A (2000) Acta Mater 48:279
2. Fan C, Inoue A (1999) Mater Trans JIM 40:1376
3. Wright WJ, Saha R, Nix WD (2001) Mater Trans JIM 42:642
4. Leng Y, Courtney TH (1991) J Mater Sci 26:588
5. Inoue A, Zhang W, Zhang T, Kurosaka K (2001) Acta Mater 49:2645
6. Donovan PE (1989) Acta Mater 37:445
7. Liu CT, Heatherly L, Easton DS et al (1998) Met Trans A 29A:1811
8. Lowhaphandu P, Montgomery SL, Lewandowski JJ (1999) Scripta Mater 41:19
9. El-Deiry PA, Vinci RP, Barbosa III N, Hufnagel TC (2001) In: Inoue A, et al (eds) Supercooled liquid, bulk glassy and nanocrystalline states of alloys, Materials Research Society, Warrendale, p L10.2
10. Xing LQ, Hufnagel TC, Ramesh KT (2001) In: Inoue A, et al (eds) Supercooled liquid, bulk glassy and nanocrystalline states of alloys, Materials Research Society, Warrendale, p L11.7
11. Flores KM, Dauskardt RH (2001) Acta Mater 49:2527
12. Zhang ZF, Eckert J, Schultz L (2003) Acta Mater 51:1167
13. Inoue A, Kato A, Zhang T, Kim SG, Masumoto T (1991) Mater Trans JIM 32:609
14. Inoue A (1995) Mater Trans JIM 36:866
15. Wert JA, Pryds N, Zhang E (2001) In: Dinesen AR, et al (eds) Proc. 22nd Riso Int. Symp., Riso National Laboratory, Denmark, p 423
16. Pryds NH, Eldrup M, Ohnuma M et al (2000) Mater Trans JIM 41:1435
17. Chen G, Ferry M (in press) J Mater Sci (accepted and in press)
18. Dieter GE (1986) Introduction to mechanical metallurgy, John Wiley
19. Berthelot JM, Fatmi L (2004) Eng Fract Mech 71:1535

20. He G, Löser W, Eckert J, Schultz L (2003) Mater Sci Eng A352:179
21. Honeycombe RWK (1985) The plastic deformation of metals. Edward Arnold
22. Flores KM, Dauskardt RH (2001) Mater Sci Eng A319–321:511
23. Wright WJ, Schwarz RB, Nix WD (2001) Mater Sci Eng A319–321:229
24. Jiang WH, Pinkerton FE, Atzmon M (2003) Scripta Mater 48:1195
25. Vaidyanathan R, Dao M, Ravichandran G, Suresh S (2001) Acta Mater 49:3781
26. Patnaik MNM, Narasimhan R, Ramamurty U (2004) Acta Mater 52:3335
27. Ramamurty U, Jana S, Kawamura Y, Chattopadhyay K (2005) Acta Mater 53:705
28. Conner RD, Johnson WL, Paton NE, Nix WD (2003) J Appl Phys 94:904
29. Murali P, Ramamurty U (2005) Acta Mater 53:1467